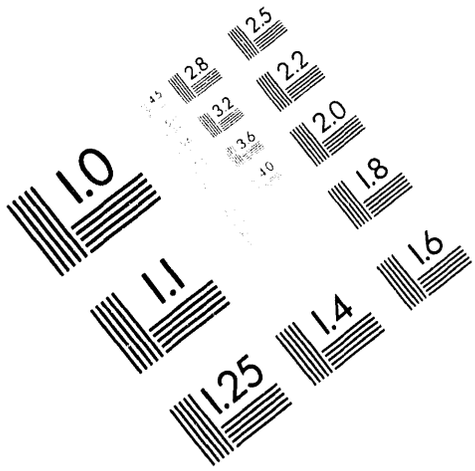

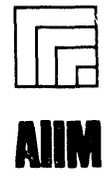

AIIM

Association for Information and Image Management

1100 Wayne Avenue, Suite 1100
Silver Spring, Maryland 20910

301/587-8202

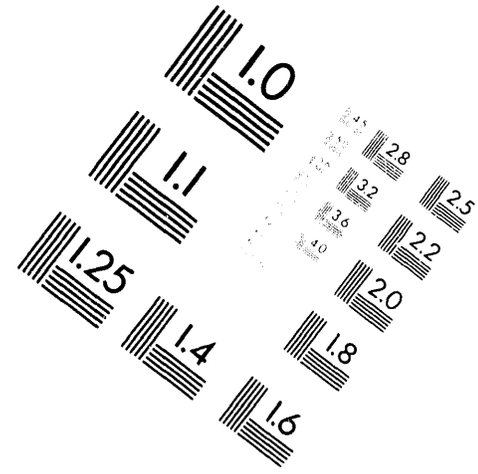

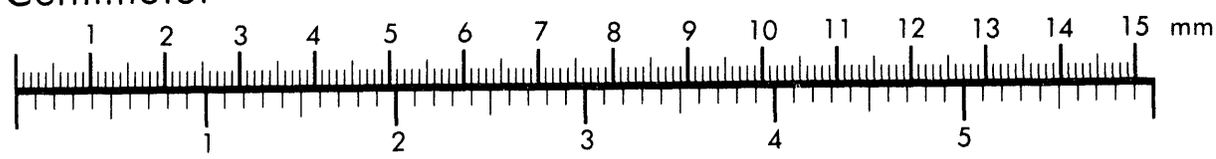

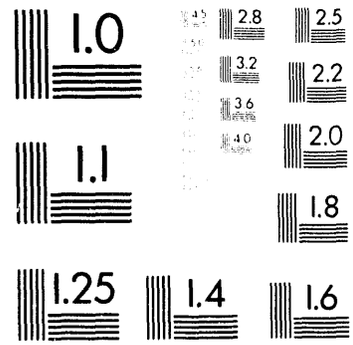

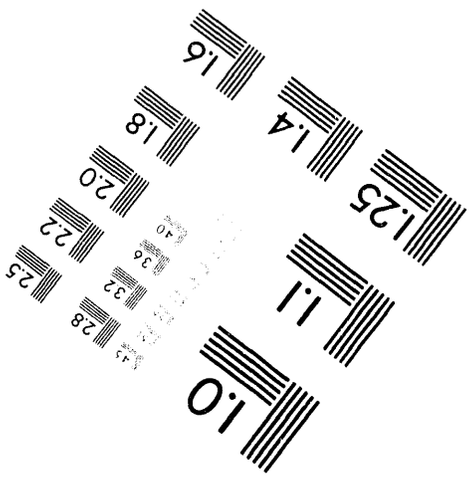

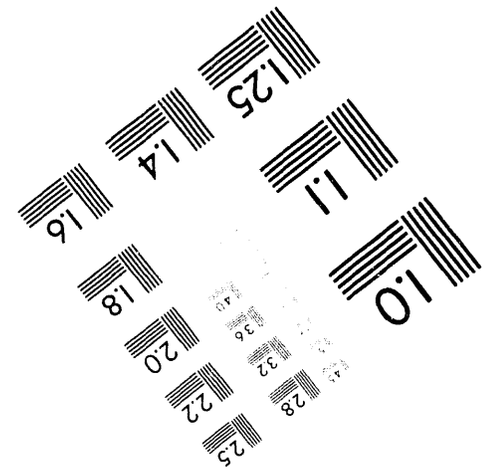

MANUFACTURED TO AIIM STANDARDS
BY APPLIED IMAGE, INC.

1 of 1

ABSORPTION OF INTENSE MICROWAVES AND ION ACOUSTIC TURBULENCE DUE TO HEAT TRANSPORT

J. S. De Groot,[1] J. M. Liu,[1] . J. P. Matte,[2] D. Perdue,[1] T. W. Johnston,[2] R. P. Drake,[3] K. G. Estabrook,[4] W. L. Kruer,[4] A. B. Langdon,[4] V. Bychenkov,[5] S. Uryupin,[5] and V. Silin[5]

January 20, 1994
UCD PRG-217
To appear in the proceedings of the 11th Laser Interaction and Related Plasma Phenomena, Monterey Calif., October, 1993

ABSTRACT

Measurements and calculations of the inverse bremsstrahlung absorption of intense microwaves are presented. The isotropic component of the electron distribution becomes flat-topped in agreement with detailed Fokker-Planck calculations. The plasma heating is reduced due to the flat-topped distributions in agreement with calculations. The calculations show that the heat flux at high microwave powers is very large, $q_{max} \approx 0.3\, n_e v_e T_e$. A new particle model to calculate the heat transport inhibition due to ion acoustic turbulence in ICF plasmas is also presented. One-dimensional PIC calculations of ion acoustic turbulence excited due to heat transport are presented. The 2-D PIC code is presently being used to perform calculations of heat flux inhibition due to ion acoustic turbulence.

1. INTRODUCTION

Inverse-bremsstrahlung absorption is dominant in the warm, long-scale-length plasmas produced when lasers irradiate high gain pellets.(1) In some pellet designs, the average ionic charge, Z, and the laser intensity are large enough that the distribution function is predicted to be non-Maxwellian (flat-topped). This has important consequences: reduction of the absorption rate,(2) the electron heat flux,(3) and the threshold of the ion acoustic drift instability,(4) and modification of the continuum X-ray emission rates(5,6) and the excitation and ionization rates.(7) Non-Maxwellian distributions are predicted(2) when the parameter $\alpha \gtrsim 1$, $\alpha = Z v_{os}^2 / v_e^2$, where v_{os} is the oscillating velocity of an electron in the electric field of the

[1]Department of Applied Science and Plasma Research Group, University of California, Davis, California 95616
[2]INRS-Energie, Canada
[3]Plasma Physics Research Institute and Department of Applied Science, University of California, Davis and Lawrence Livermore National Laboratory, Livermore, California 94550
[4]Lawrence Livermore National Laboratory, Livermore, California 94550
[5]Lebedev Institute, USSR

electromagnetic wave, $v_{os} = eE_0/m_e\omega_0$, m_e is the electron mass, ω_0 is the frequency of the electromagnetic wave, and v_e is the electron thermal speed, $v_e = \sqrt{T_e/m_e}$. In this case, the isotropic component of the electron velocity distribution is not Maxwellian but flat-topped ($f_{e0} \sim \exp\{-(v/v_m)^m\}$, with the index, $m > 2$, $v_m^2 = v_e^2\, 3\, \Gamma(3/m)/\Gamma(5/m)$, $\Gamma(x)$ is the Gamma function). For non-Maxwellian distributions, T_e is the kinetic temperature, i.e., 2/3 of the average kinetic energy.

Recently[8] we reported the first measurements of flat-topped distributions due to inverse bremsstrahlung heating by intense electromagnetic waves. It was shown that the measured results agree very well with Fokker-Planck simulations. In the first part of this paper, we present measurements and calculations of electron heating due to inverse bremsstrahlung absorption of high power microwaves. The measured results are in very good agreement with the calculations.

We recently[4] applied a new theory[9] of ion turbulence driven by heat transport to laser plasmas driven by high laser powers. We showed that the threshold can be exceeded for high laser powers in high Z plasmas - conditions that can occur in indirectly driven ICF plasmas. The heat flux is only weakly limited if the isotropic part of the electron velocity distribution function is Maxwellian. However, the heat flux is strongly limited if the isotropic part of the electron velocity distribution function is strongly non-Maxwellian ($f \approx \exp(-v^5)$). In the second part of this paper, we present a new particle simulation model that is presently being used to calculate the heat transport inhibition due to ion acoustic turbulence. Previous simulation calculations of the ion acoustic drift instability have involved imposing an electric field and measuring the time dependent current or imposing an external circuit that maintains a constant current. The problem with this approach is that the ion acoustic turbulence develops and then is damped by suprathermal ions that are accelerated by the turbulence. This is the origin of the widely held view that in steady state the turbulence level and anomalous resistivity is much less than theoretical estimates.[9] The point is that the level of the steady state turbulence is a strong function of the boundary conditions. We have developed a new PIC model that is applicable to laser heated plasmas. The appropriate boundary conditions for laser driven plasmas are periodic in the y direction and bounded in the x direction. Electrons and ions are injected into and exit from the plasma. The particles heated by the turbulence are therefore replaced by thermal particles. Finally, we present the first PIC calculations of ion acoustic turbulence excited due to heat transport.

2. INVERSE BREMSSTRAHLUNG ABSORPTIONOF HIGH POWERED MICROWAVES

2.1. Experimental Device

The experiments are performed in the UCD AURORA II device, an improved version of the UCD AURORA device.[10] The improvements are: higher plasma

fractional ionization, higher microwave power, a variable density gradient, and a greatly improved data acquisition and analysis system.. A schematic diagram of the AURORA II device is shown in Figure 1.

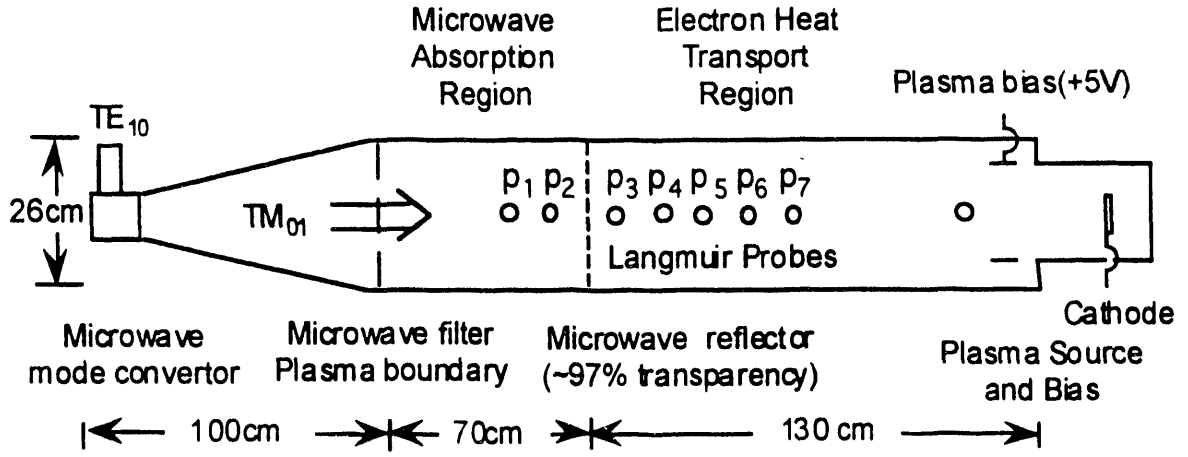

Figure 1. Schematic diagram of the AURORA II. device

The plasma is created by a pulsed discharge in low pressure argon (P ~ 0.3 mTorr, neutral density, $n_{argon} \sim 10^{13}$ cm^{-3}). The argon pressure is low enough that the high power microwaves do not significantly increase the fractional ionization. Permanent magnets are arranged on the surface of the cylindrical vacuum chamber to increase the fractional ionization (~ 1%) and to produce an axial plasma density gradient. The axial density gradient is controlled by biasing anodes that are placed along the discharge length. The plasma is bounded axially (z = 0) by a metal sheet with a small annular opening that serves as a microwave filter. A microwave reflector (transparency ~ 97%) divides the 200 cm long plasma axially into a short microwave absorption region (length = 70 cm) and a longer heat transport region (length = 130 cm). At the time of the heating experiment, the plasma density increases approximately linearly with axial position. The critical density is reached at z ≈ 150 cm. The microwaves are excluded from the critical density region by the reflector so collective phenomena that would otherwise occur near the critical surface do not effect the results discussed here.

The microwave heating experiments are performed in the afterglow plasma. The electron density is monitored and the microwave pulse is initiated when the density decays to a preset value (typically $n_e \sim n_{max}/2$). By then, the afterglow temperature has decreased to T_{e0} = 0.4 eV, so that electron-charged particle collisions are strongly dominant over electron-neutral collisions, and the electron distribution is Maxwellian. A short microwave pulse (vacuum wavelength, λ_0 = 10 cm, frequency, f_0 = 3.0 GHz, critical density, $n_{cr} = 1.1 \times 10^{11}$ cm^{-3}, and pulse width ~ 2 μs) heats the plasma in the absorption region ($n_e/n_{cr} \lesssim 0.5$). The microwaves are transported in a rectangular waveguide (TE_{10} mode) and converted to the circular TM_{01} mode. A conical section transforms this mode adiabatically so that the plasma filled vacuum vessel is the cylindrical waveguide. A microwave filter is placed at

the entrance to the absorption region so that only the TM_{01} mode interacts with the plasma. The microwave power can be varied up to P_M = 90 kW so that, $\alpha_0 = Zv_{os}^2/v_{e0}^2 \lesssim 1.6$ (using the initial electron temperature, the electric field of the incident microwaves, $E_0 = \sqrt{8\pi P_M/Ac}$, A is the area of the waveguide, and Z = 1). Ion acoustic turbulence is not significant in our present experiments because the decay time of the electron heat flux is shorter than the growth time of the ion acoustic drift instability. Several cylindrical Langmuir probes (P_1 through P_7 in Figure 1) are placed with their axis perpendicular to the plasma axis, so that the isotropic component of the electron velocity distribution function is measured. The electron temperature, T_e, density, n_e, and distribution function index, m, are obtained by fitting the data to probe theory[11,12] that is modified to include flat-topped velocity distributions. A large signal to noise ratio (> 100) results in quite good measurement accuracy (± 7% for T_e and ±3% for m).

2.2. Fokker-Planck International Computer Code

The plasma behavior was modeled with our one dimensional electron kinetic code "FPI".[5,10,13] In the calculations, the expansion of the pitch angle dependence of the electron velocity distribution was expanded to third order in Legendre polynomials. The code includes: transport (for each energy group), a self-consistent electric field to ensure quasi-neutrality, electron-electron and electron-ion collisions in the Fokker-Planck approximation, and a kinetic heating operator[2] that is used to calculate the collisional absorption of the microwaves. Hydrodynamics was ignored in the calculations because the decay time of the heat flux is shorter than the hydrodynamic time. The electromagnetic wave equation for the TM_{01} mode was solved (using the measured plasma density profile, but neglecting the weak absorption) to find the quiver energy in the absorption region. The quiver energy was volume-averaged over the radial coordinate to produce an axial profile of the quiver energy that is used to evaluate the heating operator in the "FPI" code. It was not necessary to correct for finite v_{os} in the heating operator[14] since the parameter $\alpha_0 \lesssim 3$. A least square fit of the form $\exp(-(v/v_m)^m)$ was used to extract the index m from the "FPI" results.

2.3. Experimental Results

The distribution function index, m, and the electron temperature, T_e, in the absorption region (z = 62.5 cm) are shown in Figures 2 and 3 as a function of microwave power. The measured results (symbols) are in very good agreement with "FPI" calculations (solid lines). These data were taken in the absorption region (z = 62.5 cm) a short time (0.4 μs) after the microwave pulse. The "FPI" calculations show that the temperature and index have not decreased significantly during this time interval. The measured results also agree fairly well with a theoretical prediction[5] (dotted line in Figure 2), $m = 2+3/(1 + 1.66/\alpha^{0.724})$, here, the measured electron temperature was used to calculate α.

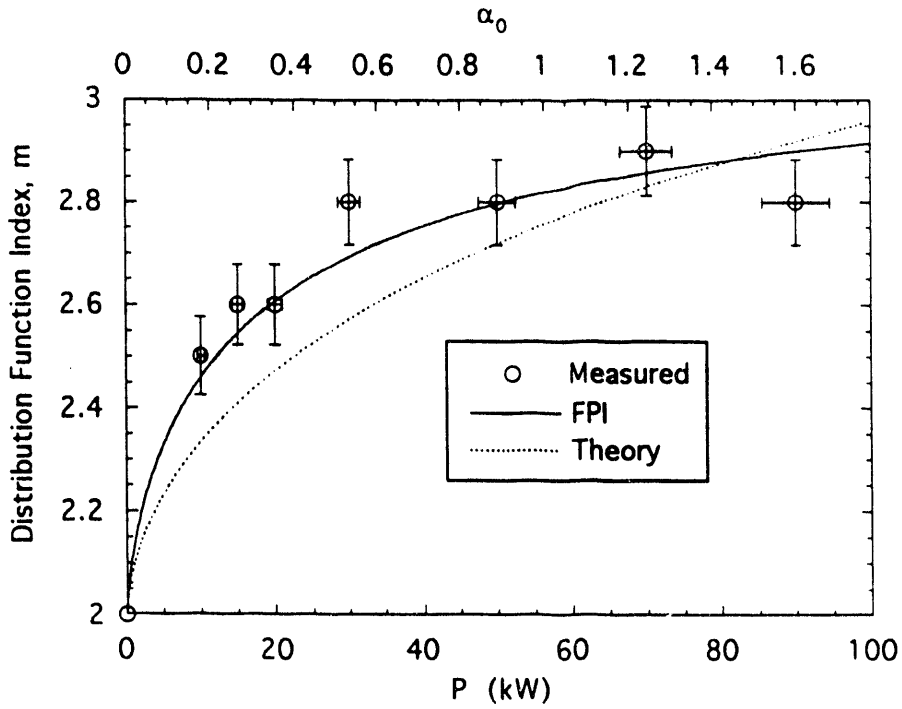

Figure 2. The distribution function index, m, as a function of microwave power. The measured values (symbols) agree very well with Fokker Planck calculations (FPI) and fairly well with a simple theory based on previous calculations (see text).

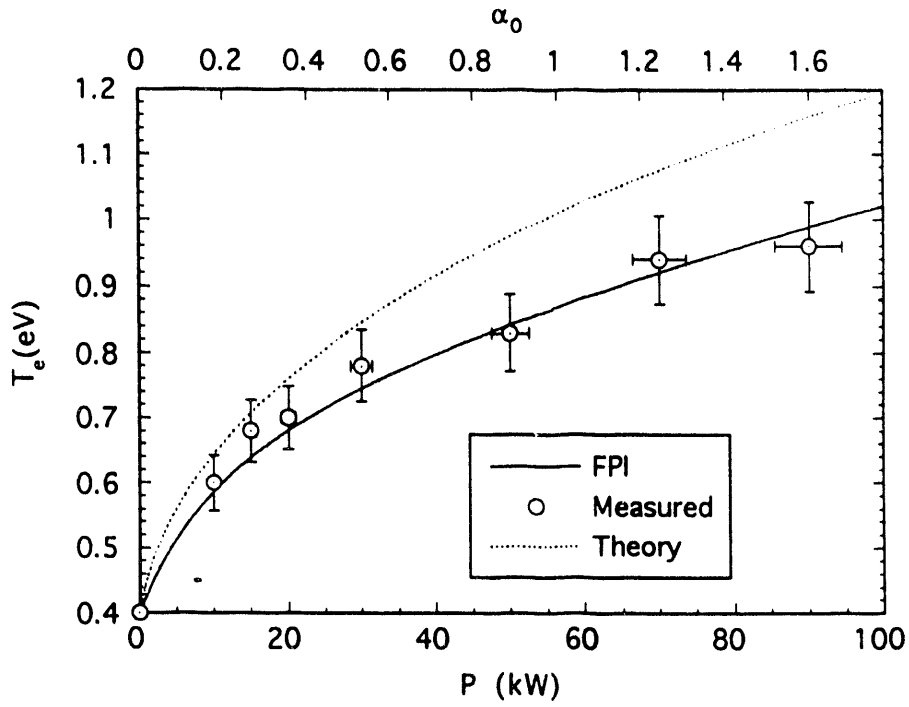

Figure 3. The electron temperature, T_e, is shown as a function of microwave power. The measured results (circles) agree with 'FPI' calculations (solid line) but disagree with theory neglecting the absorption reduction factor (dotted line, see text).

The microwave absorption is significantly reduced at high microwave powers due to the flat topped electron distribution. The absorption reduction factor[2] for a homogeneous electric field is R ≈ 0.63, for microwave power, P = 90 kW, ($R = 1 - 0.553/(1+(0.27/\alpha)^{0.75})$), and the measured electron temperature was used to calculate α). Using the measured results to determine the constants, we constructed an approximate theory for the electron temperature. The approximate theory agrees very well with the "FPI" results. The predicted electron temperature neglecting the absorption reduction factor (dotted line) does not agree with measurements, as expected.

The microwave pulse is short enough that the heated electrons predominately remain in the absorption region during the pulse. A steep temperature gradient and a very large heat flux is therefore created near the boundary between the absorption region and the heat transport region. The maximum heat flux from "FPI" calculations is shown in Figure 4 as a function of microwave power. A heat flux as large as $q = 0.32\, n_e v_e T_e$ is predicted for our experiment at a power of 90 kW. Based on our previous theory,[4] this would result in an effective velocity of return current of $u_{eff} \sim 4\, C_s$. This is well above the threshold for the excitation of ion acoustic waves, so ion acoustic turbulence would be excited in our experiment. However, the microwave pulse is sufficiently short that the heat flux decays before the ion acoustic waves can grow significantly.

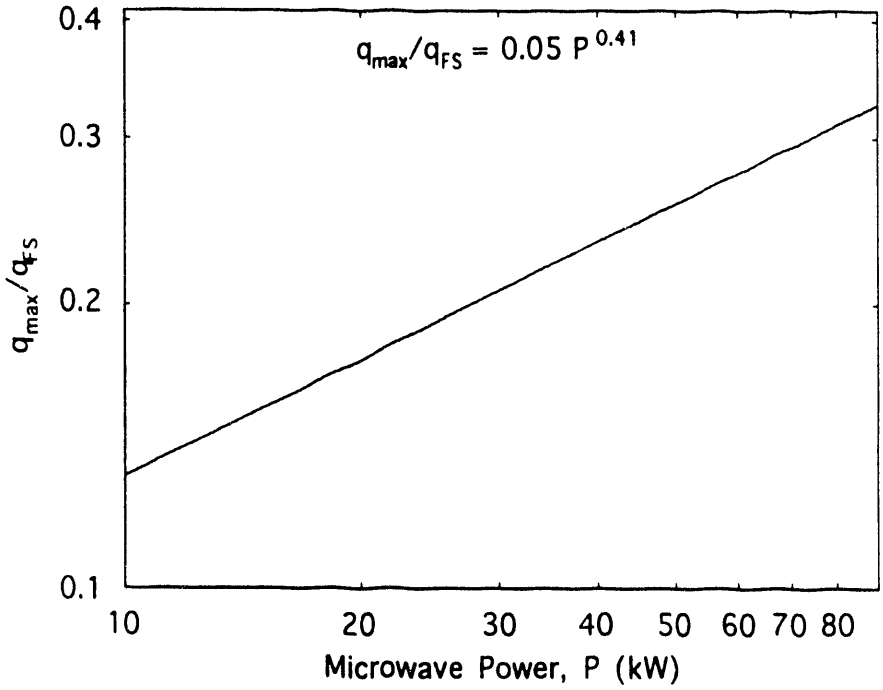

Figure 4. "FPI" calculations of the maximum heat flux as a function of microwave power.

3. PARTICLE SIMULATION CALCULATIONS OF INHIBITED HEAT TRANSPORT DUE TO ION ACOUSTIC TURBULENCE

We have developed a new computational model to calculate the heat transport inhibition due to ion acoustic turbulence. We have incorporated this model into the 1-D, 2 velocity (v_x and $v_\perp$) PIC code HEAT and the 2-D, 3 velocity, PIC code HEAT2. The simulation region is a small section ($x_{max} \sim 200\ \lambda_{De}$) near the maximum heat flux in an ICF pellet. The simulated plasma is connected to a lower temperature plasma at the left boundary, $x = 0$ and a higher temperature plasma at the right boundary, $x = x_{max}$. Particles that leave the system in the x-direction are re-injected into the plasma with an energy distribution that is characteristic of the bounding plasmas. The initial plasma density and fluid velocity are chosen so that the system is in hydrodynamic equilibrium. Electron-ion collisions are modeled using the Shanny-Dawson-Green[15] collision model (Lorentz model, $M \rightarrow \infty$).

Results from HEAT are shown in Figures 5 and 6. The main parameters for this run were: plasma length = 100 λ_{De}, ratio of right to left boundary temperature = 2, number of electrons = number of ions = 16k , electron mass/ion mass = 400, and electron temperature/ ion temperature = 25. This calculation was performed without the collision model. The electron velocity distribution at the end of the calculation is shown in Figure 5. A drifting Maxwellian distribution least squares least squares fit is also shown. The effective drift velocity of the return current electrons is about $v_{eff} \approx 2\ C_s$, so ion acoustic waves should be unstable (since T_e/T_i = 25).

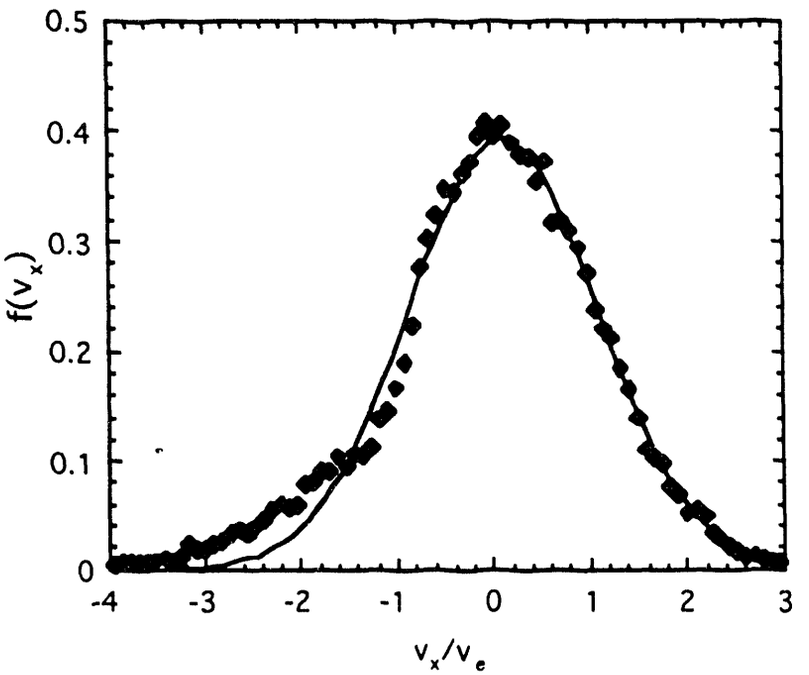

Figure 5. The electron velocity distribution, $f(v_X)$, at the end of the calculation.

The time history of the amplitude of the Fourier analyzed ion density (mode 8, $k\lambda_{De} \approx 0.44$) is shown in Figure 6. Mode 8 grows the fastest in agreement with theory. As expected, the ion acoustic waves do not grow if the temperature ratio is decreased or the heat flux is decreased so that the return current is below the threshold.

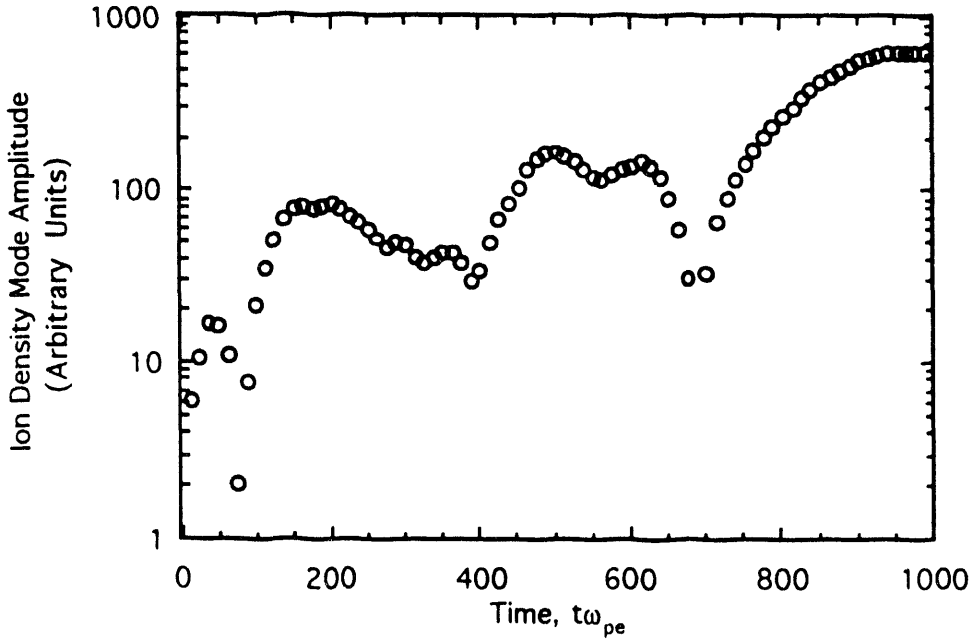

Figure 6. Ion density amplitude as a function of time. Mode 8 ($k\lambda_{De} \approx 0.44$) is shown.

4. SUMMARY

We presented measurements and calculations of the inverse bremsstrahlung absorption of intense microwaves. The isotropic component of the electron distribution becomes flat-topped in agreement with detailed Fokker-Planck calculations. The plasma heating is reduced due to the flat-topped distributions in agreement with the calculations. The calculations show that the heat flux at high microwave powers is very large, $q_{max} \approx 0.3\, n_e v_e T_e$. We also presented a new particle model to calculate the heat transport inhibition due to ion acoustic turbulence in ICF plasmas. Using the new model, it was shown that ion acoustic turbulence was excited due to heat transport. We are presently using the 2-D code to perform calculations of heat flux inhibition due to ion acoustic turbulence.

Acknowledgments

The authors gratefully acknowledge fruitful discussions with J. H. Rogers. We would like to thank T. Hillyer, H. Bandeh, and A. Froeschner for their technical support. This work was sponsored by the Plasma Physics Research Institute, the Lawrence Livermore National Laboratory and was partially performed under the

auspices of the U.S. Department of Energy by the Lawrence Livermore National Laboratory under Contract W-7405-Eng-48.

REFERENCES

1. W. L. Kruer, Comments on Plasma Physics and Controlled Fusion **5**, 69 (1979).
2. A. B. Langdon, "Nonlinear Inverse Bremsstrahlung and Heated Electrons," Physical Review Letters, **44**, 575 (1980).
3. P. Mora and H. Yahi, Physical Review A, **26**, 2259 (1982).
4. J. S. De Groot, K. G. Estabrook, W. L. Kruer, R. P. Drake, K. Mizuno, and S. M. Cameron, *Distributed Absorption and Inhibited Transport*, Proceedings of the 10th Workshop on Laser-Plasma Interactions and Related Phenomena, Monterey, Calif., Nov. 1991 **10**, 197 (1992).
5. J. P. Matte, M. Lamoureux, C. Moller, R. Y. Yin, J. Delettrez, J. Virmont, and T. W. Johnston, "Non-Maxwellian Electron Distributions and Continuum X-Ray Emission in Inverse Bremsstrahlung Heated Plasmas," Plasma Physics and Controlled Fusion, **30**, 1665 (1988).
6. D. L. Matthews, R. L. Kauffman, J. D. Kilkenny and R. W. Lee, Applied Physics Letters **44**, 586 (1984).
7. P. Alaterre, J. P. Matte and M. Lamoureux, "Ionization and Recombination Rates in Non-Maxwellian Plasmas," Physical Review A **34**, 1578 (1986).
8. J. M. Liu, J. S. De Groot, J. P. Matte, T. W. Johnston, and R. P. Drake, "Measurements of Inverse Bremsstrahlung and non-Maxwellian Electron Velocity Distributions," Submitted to Physical Review Letters, 1993.
9. V. Yu. Bychenkov, V. P. Silin, and S. A. Uryupin, "Ion Acoustic Turbulence and Anomalous Transport," Physics Reports, **164**, 119 (1988); V. Yu. Bychenkov, V. P. Silin, and S. A. Uryupin, Comments on Plasma Physics and Controlled Fusion, **13**, 239 (1990).
10. J. H. Rogers, J. S. De Groot, Z. Abou-Assaleh, J. P. Matte, T. W. Johnston, and M. D. Rosen, "Electron Heat Transport in a Steep Temperature Gradient," Physics of Fluids B **1**, 741 (1989).
11. J. D. Shift and M. J. R. Schwar, Electrical Probes for Plasma Diagnostics, (American Elsevier Publishing Company, Inc. New York, 1969).
12. J. H. Rogers, J. S. De Groot and D. Q. Hwang, "Validing Cylindrical Langmuir Probe Techniques," Review of Scientific Instruments, **63**, 31 (1992).
13. J. P. Matte, T. W. Johnston, J. Delettrez and R. L. McCrory, "Electron Heat Flow with Inverse Bremsstrahlung and Ion Motion," Physical Review Letters, **53**, 1461 (1984).
14. L. Schlessinger and J. Wright, "Inverse-Bremsstrhlung Absorotion Rate in an Intense Laser Field," Physical Review A **20**, 1934 (1979).
15. R. Shanny, J.M. Dawson, and J. M. Greene, "One-Dimensional Model for a Lorentz Plasma," Physics of Fluids, **10**, 1281 (1967).

Doc I

DATE FILMED

8/18/94

END